The College of Engineering
University of Wisconsin-Madison

Wisconsin Electric Machines and Power Electronics Consortium

RESEARCH REPORT
93-61

Analysis of Concentrated Winding Induction Machines for Adjustable Speed Drive Applications-Experimental Results

Hamid A. Toliyat
Fedowsi University-Mashhad
P.O. Box 91775-1863
Mashhad, Iran

Thomas A. Lipo
Dept. of Electrical and Computer Engineering
University of Wisconsin-Madison
1415 Johnson Drive
Madison, WI 53706

WEMPEC

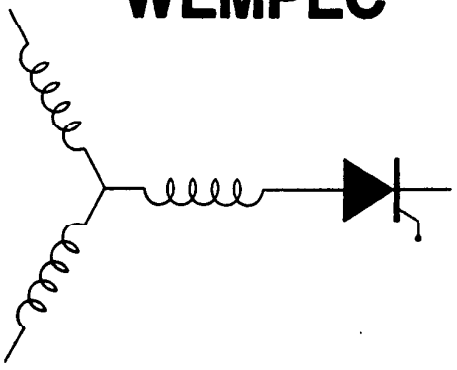

Department of Electrical and Computer Engineering
1415 Johnson Drive
Madison, Wisconsin 53706

Analysis of Concentrated Winding Induction Machines for Adjustable Speed Drive Applications-Experimental Results

Hamid A. Toliyat
Member, IEEE
Ferdowsi University-Mashhad
P.O. Box 91775-1863
Mashhad, Iran

Thomas A. Lipo
Fellow, IEEE
University of Wisconsin-Madison
1415 Johnson Drive
Madison, WI 53706

Keywords: Concentrated Winding, Adjustable Speed Drive, Induction Machines, Test Results

Abstract - The approach to analysis of multiphase concentrated winding induction machines specifically designed for operation with static power converters derived in [1], is implemented by means of a digital computer simulation in [2]. In order to substantiate the theoretical conclusions regarding the performance of the multiphase induction motors an experimental five phase induction motor and its corresponding converter and control are designed and fabricated. In this paper some of the design criteria and the experimental results obtained from the test will be presented and analyzed.

Introduction

In [1] the differential equations of an m phase induction machine with concentrated full pitch windings were derived. This model is based on coupled magnetic approach by considering that the current in each bar is an independent variable. The effects of non-sinusoidal air-gap MMF produced by both the stator and the rotor currents have been incorporated into the model. In [2] the equations derived in [1] were implemented on a digital computer. Computed results show that when operating in conjunction with a converter supply which each semiconductor switch carries a 144 degree block of current, a specifically wound five phase machine is theoretically capable of a 10% improvement in torque per rms ampere assuming the same peak air-gap flux density level in the air-gap of the machine as in a conventionally designed induction motor of the same rating [3]. In this paper the experimental results achieved from the test will be given and analyzed. The correlations and discrepancies versus the theoretical predictions of the five phase induction motor will also be discussed.

Design of the Experimental Five Phase Induction Motor

The five-phase induction motor [4] designed and fabricated is a standard frame of a 7.5 hp, 4 pole, 60 Hz, 460 V, three phase induction motor. The decision to build the five phase induction motor on this frame is based on the availability of the three phase, four pole version in the lab and therefore, the possibility of an experimental comparison between the two machines. The original three phase, four pole, 7.5 hp induction motor has 36 stator slots and 28 rotor bars. The rotor is skewed by one rotor slot. The stator is double layer with a pitch equal to 8/9. To have a fair comparison the five phase machine should have the same amount of copper and iron. Since the five phase induction motor proposed has concentrated windings and full pitch, the respective number of stator slots will be 10 for a two pole, 20 for a four pole and 40 for an eight pole and so on. The 40 stator slots was chosen due to the fact that it has a good cooling capability. However, because of the cost involved in the laser cut of the designed slot, a smaller slot was chosen. Therefore, the effective magnetic material of the five phase machine is a little bit higher than the three phase noting that this increase in the magnetic material mainly exists in the back iron.

The material of the stator laminations chosen is grade M-45 and gauge #26, which is similar to the original three phase machine. It is important to mention that M-45 iron has a very low silicon content as well as low cost. The general application of M-45 material is suggested only for intermittent rotating machines, pole pieces or relays. The stator slot is a typical round bottom semi-opened slot for low horse power ac machines to accommodate round wire in random style.

Since the total number of turns were kept the same the amount of copper used in this machine is less than the three phase conventional wound machine, due to the fact that it has shorter end turns (because of more poles) and smaller stator slots. The same laminations and the same copper wire was used. The total number of turns was kept the same. To prevent the air gap flux from distortion by the skew of the rotor, a similar 28 bars rotor without skew was designed and built. The machine is wound with 54 turns of double strand gauge #19 copper wire. Since the machine is eight pole and full pitch, there are four circuits and these circuits are connected in parallel to have a lower terminal voltage. Therefore, the converter needs less bus voltage to be able to regulate the prescribed current in the machine. The fully pitched winding does not become a problem because the space harmonics are utilized in the torque production. However, the end winding part of the full pitched winding is higher than the short pitched winding.

The winding layouts for the original three phase, four pole, 36 stator slots and the designed five phase, eight pole, 40 stator slots are given in Figure 1. The terminal connection of the three phase machine was modified such that all four circuits were connected in parallel to match the converter bus voltage at rated current and speed.

Design of the Five Phase Current Regulated PWM

The current regulated PWM inverter [5] consists of a conventional PWM voltage source inverter with current regulating loops to provide a controlled current output. Since the inverter has a rather high switching frequency, the stator currents of the induction motor can be rapidly adjusted in magnitude and phase. There are benefits arising from the operation of the converter as a controlled current

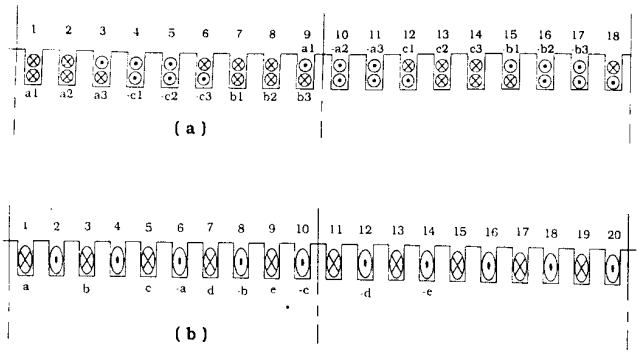

Figure 1 *Winding layout for a) three phase, double layer, four pole, b) five phase, concentrated winding, eight pole stator of induction motors.*

source such as inherent short circuit protection, and there are no transient current surges, so that a more economical inverter design is possible. Also, since the motor torque is determined by the air-gap flux and machine current, an improved dynamic performance is achieved by directly controlling the stator current rather than the terminal voltage. There are different type of current regulators used to control the current.

In one method [6,7] known as Hysteresis Current Regulator a reference current waveform is generated and fed to a comparator, together with the actual measured current of the motor. The simplest method uses the comparator error to switch the devices in the inverter half bridge so as to limit the instantaneous current error. In case that the motor phase current is more positive than the reference current value, the upper device is turned off and the lower device is turned on and vise versa. The comparator has a hysteresis band that determines the permitted deviation of the actual phase current from the reference value before an inverter switching is initiated. The smaller the hysteresis band is, the higher the switching frequency should be. However the switching frequency is not constant for a given hysteresis band and is modulated by the variations in motor inductance and back EMF. There are potential problems with this current regulator, i.e. the switching frequency may rise excessively when the back EMF is low and also the instantaneous current error can reach double the hysteresis band. Also, the variable switching frequency produces objectionable acoustic noise. This current regulator was implemented in the lab and due to the above mentioned reasons its further use was abandoned.

In another method called Fixed Frequency Current Regulator the current error is compared with a fixed frequency triangular carrier wave. The resulting PWM signal with the duty cycle proportional to the current error, controls the switching. Similar to the previous case, when the reference current is more positive than the actual current, the resulting error is positive and the on period of the upper device exceeds that of the lower device. Therefore, the inverter leg is switched predominantly in the positive direction to increase the ac line current. Similarly, in case that the current error is negative, the inverter leg is switched predominantly in the negative direction.

Figure 2 shows the block diagram representing this type of current regulator. The current comparison is done in a linear operational amplifier current controller with proportional or proportional plus integral compensation. The compensation is adjusted to minimize the magnitude and phase errors in the machine line currents. By feeding the induction motor with impressed stator currents, the effects of stator resistance and leakage reactance are eliminated, and it is easy to control the induction motor performance.

In a wye connected induction motor with isolated neutral, the summation of ac line currents must add up to zero. Therefore, it is sufficient to sense and control the currents in all the lines minus one. For proper operation of the inverter as a controlled current source, the dc link voltage must be sufficiently large to force the ac line currents to vary as prescribed. When the motor speed rises, the back EMF increases and approaches the dc link voltage and as a result the output current is unable to track the reference current.

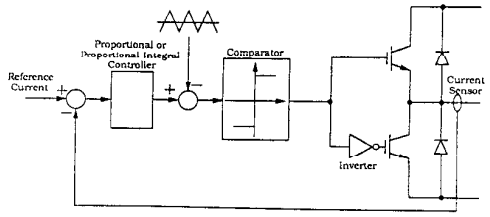

Figure 2 *The fixed frequency current regulator control for one inverter leg.*

CONTROLLED CURRENT OPERATION

An important limitation of the current regulated PWM is the fact that open loop operation in the manner of a voltage source inverter is not possible. Figure 3 shows the torque speed of a typical induction motor fed from both a voltage source and a current source inverter [8]. If the magnetizing inductance is assumed to be constant, and the motor is current fed with rated stator current at rated frequency, then the developed torque builds up from a very low value at standstill to a breakdown value and then falls down rapidly to zero at synchronous speed.

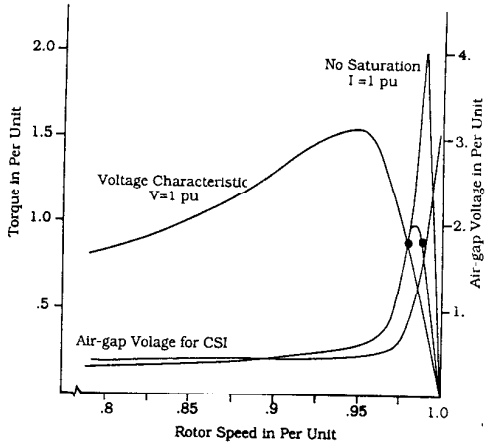

Figure 3 *Torque speed curves for current controlled and voltage controlled induction motor.*

This phenomena is explained by the corresponding air gap voltage curve which indicates that the air gap flux is very small near standstill. The reason is that at standstill the slip is large and therefore the low value of referred rotor impedance limits the air gap voltage developed by the rated stator current. As the motor speeds up, the rotor impedance and air gap voltage increase, allowing the development of greater flux and torque. Near the synchronous speed, the motor is highly saturated and the assumption of a constant magnetizing reactance is not justified and the torque is smaller.

Inspection of the Figure 3 suggests two possible operating points, one on the negatively sloped region which is the stable points and one on the positively sloped region which is the unstable operating point. Operation on the stable side is not possible because the air gap flux and core losses are larger and the terminal voltage is higher. However, operation on the unstable side results in the rated air gap flux but, this mode of operation requires a feed back loop. The motor torque is varied by adjusting the stator current and rotor frequency so that rated air gap flux is maintained. Therefore, the motor operating points fall on the torque speed curve defined for rated voltage operation.

Figure 4 is a block diagram of a five phase current regulated PWM. The speed command, n^*, is rate limited by a ramping circuit before defining the inverter frequency reference, ω_1^*, in a simple open loop control. The frequency command also specifies a proportional stator voltage command, V_1^*, and therefore a constant volts/hertz ratio. The terminal voltage of the motor is rectified by a diode rectifier bridge and filtered before being compared with the commanded voltage. The error signal from the voltage controller develops the appropriate current amplitude command, I_1^*. Thus, the motor current is adjusted to a level that develops the commanded terminal voltage, and the air gap flux level is approximately constant if stator resistance effects are small. A low frequency voltage boost can be introduced by adding a voltage offset to the frequency proportional voltage reference.

The two command signals, I_1^* and ω_1^*, control the amplitude and frequency of the five phase reference waveform currents delivered by the reference waveform generator. These signals can be generated digitally by storing the reference wave look up tables in ROM. The stored values are read at a rate determined by the stator frequency command, ω_1^*. The digital output signal is then converted to analog form by a multiplying digital to analog converter (MDAC) which are compared with the actual motor currents. Note that in Figure 4 only four phase currents need be directly measured since $i_a+i_b+i_c=0$. The block labeled PWM Gen represents the fixed frequency current regulator that generates the PWM firing signals for the inverter leg.

In the constant torque region, the functional relationship between I_1^*, ω_1^* is such that rated magnetizing current is flowing in the machine. Field weakening can be implemented by modifying the output of the voltage controller. The current regulated PWM drive with a voltage feedback loop can operate stably in the region corresponding to the rated air gap flux condition.

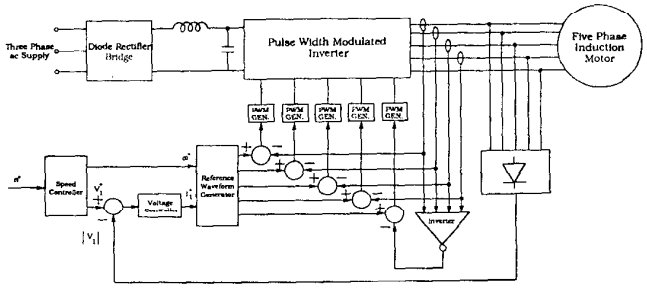

Figure 4 *The five phase current regulated PWM inverter drive with stator voltage feedback.*

Experimental Results of the Three Phase Induction Motor

The three phase, four pole, conventionally wound induction motor with the multiphase current regulated PWM converter described in the previous sections were tested in the lab. The results are given in this section. The machine contained a search coil placed in the stator slot opening. The voltage induced in this search coil under no load and locked rotor conditions were integrated to obtain the flux linkages. Assuming that the flux in the stator tooth is uniformly distributed, dividing the total flux entering a tooth, by its area results in the tooth flux density.

No Load Test

The three phase machine was operated at no load. The line to line rms voltage, phase rms current, power factor between the line voltage and phase current as well as the stator tooth flux were recorded.

Figure 5 and 6 show the oscilloscope viewgraph at about 50% and 140% of the rated magnetizing current corresponding to unsaturated and saturated conditions respectively. Notice that due to the high speed and current the induced back EMF of the machine is comparable to the converter bus voltage and because of insufficient dc bus voltage (250 V), it is clear that the current regulation is not very good. Due to the fact that the machine is sinusoidally wound, a rather sinusoidal flux waveform appears, at even low current which the machine is less saturated. However, at high current because of saturation effect, the addition of the third harmonic in the flux wave is clear. The bottom

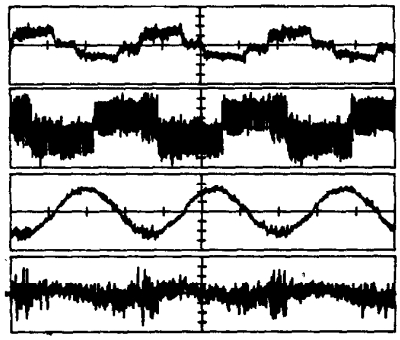

Figure 5 *Oscillogram of the three phase machine at no load, rms phase current=5A, f=30 Hz, a) Phase current (5 A/div.), b) Line voltage (100 V/div.), c) Stator tooth flux density (.2 T/div.), d) Stator tooth search coil voltage (.5 V/div.)*

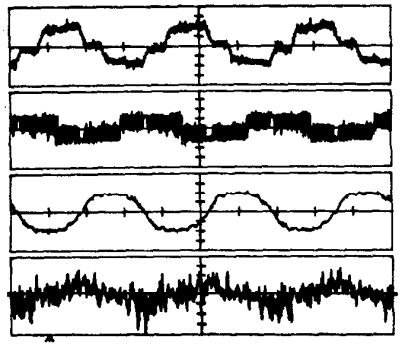

Figure 6 *Oscillogram of the three phase machine at no load, rms phase current=11A, f=30 Hz, a) Phase current (5 A/div.), b) Line voltage (100 V/div.), c) Stator tooth flux density (.5 T/div.), d) Stator tooth search coil voltage (.5 V/div.)*

trace in Figure 6 depicts the search coil voltage showing the effect of slot ripples. In this case because of higher current than in Figure 5, the search coil voltage is higher and therefore the effect of slot ripples are more profound.

Locked Rotor Test

Figure 7 illustrates the oscillogram for locked rotor test. In this case since rotor current exists, the flux density in the stator tooth is the total flux produced by the stator windings and the rotor cage. The six step operation can be observed in the flux density waveform. The shaft was locked with a locking device and the machine was supplied at a frequency of 2.825 Hz, which corresponds to the rated slip frequency. A high frequency signal due to the switching frequency of the converter overriding it, is also detectable. Steady state torque was obtained from a shaft mounted torque transducer.

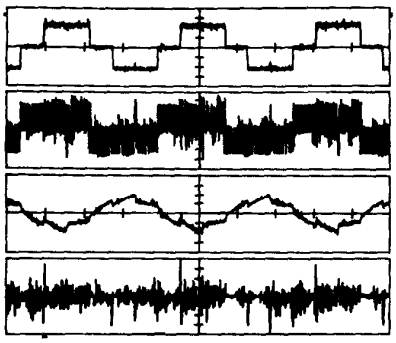

Figure 7 *Oscillogram of the three phase machine at locked rotor, rms phase current=18A, f=2.825 Hz, a) Phase current (10 A/div.), b) Line voltage (100 V/div.), c) Stator tooth flux density (.5 T/div.), d) Stator tooth search coil voltage (.2 V/div.)*

EXPERIMENTAL RESULTS OF THE FIVE PHASE INDUCTION MOTOR

The five phase, eight pole, concentrated winding induction motor with the multiphase current regulated PWM inverter described in the previous sections were tested in the lab. The results are given in the next two sections. The machine contained a search coil placed in the stator slot which after integration results in the tooth flux linkages, and also another one parallel to the phase winding to determine the total flux linking one stator phase per pole pair. This search coil was placed in the slots 1 and 6.

No Load Test

Similar to the method presented before, the no load test was performed at about 50% and 140% of rated magnetizing current of induction motor. The results are depicted in Figures 8 and 9 which correspond to unsaturated and saturated conditions respectively. However, since the terminal voltage of the five phase machine is less than the terminal voltage of the three phase induction motor, the bus voltage is capable of regulating the winding current to the prescribed waveform. Due to the nature of stator coils, which are full pitch and concentrated, the stator tooth flux density is not sinusoidal and takes rather a trapezoidal waveform. Again since at 140% of rated magnetizing current, the search coil voltage is high enough with respect to the induced voltage due to the switching, the slot ripples are more obvious. Notice the presence of the third harmonic in the machine phase voltage.

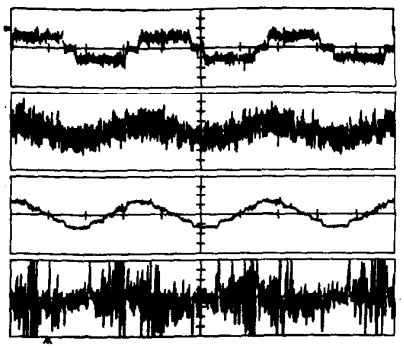

Figure 8 *Oscillogram of the five phase machine at no load, rms phase current=5A, f=30 Hz, a) Phase current (5 A/div.), b) Line voltage (100 V/div.), c) Stator tooth flux density (.5 T/div.), d) Stator tooth search coil voltage (.1 V/div.)*

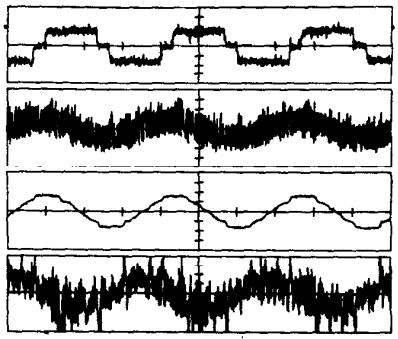

Figure 9 *Oscillogram of the five phase machine at no load, rms phase current=14A, f=30 Hz, a) Phase current (10 A/div.), b) Line voltage (100 V/div.), c) Stator tooth flux density (1.0 T/div.), d) Stator tooth search coil voltage (.1 V/div.)*

To verify the validity of the simulation results presented in the previous papers [1,2], the stator phase flux linkages is calculated and compared with the experimental results. Shown in Figure 10, top trace, is the total flux linking one stator phase achieved by digital computer. The machine is running at no load with rated magnetizing current. The input current waveform is the 144 degree quasi square waveform at 60 Hz. The bottom trace depicts the flux linking a pole by inserting a search coil in the 1st and 6th stator slots. This result is obtained by integrating the induced voltage in the search coil using an active integrator and viewing it on a digital oscilloscope. The measured and calculated waveform agree very well. Notice the presence of the high frequency signal due to the switching frequency in the measured oscillogram.

Locked Rotor Test

Figure 11 depicts the oscillogram for locked rotor test. Similar to the three phase locked rotor test, the shaft is locked with a plier. The operating frequency is 2.825 Hz which is about the rated slip frequency. The effect of existing rotor current in the stator tooth flux density is evidenced. Since the back EMF is negligible, the phase voltage is assuming more of a square waveform rather than a sinusoidal waveform which was existed in the no load test shown in Figures 8 and 9. Again the stator rms current was varied and the steady state torque was recorded using a shaft mounted transducer.

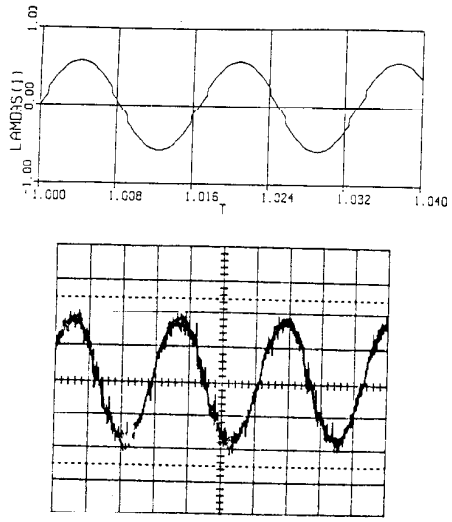

Figure 10 *Comparison of calculated and measured stator flux linkages at no load. Top trace, digital computer result in volts.sec. Bottom trace, test result with .25 V/div. and 5 msec./div.*

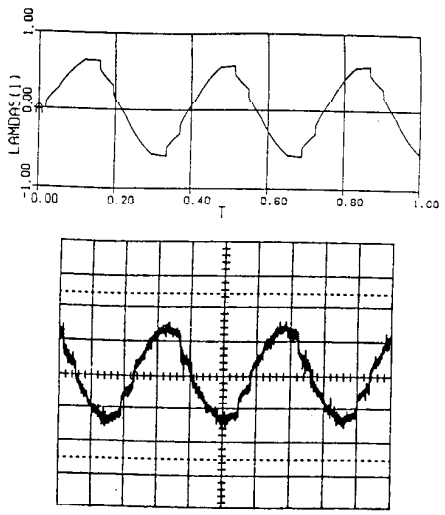

Figure 12 *Comparison of calculated and measured stator flux linkages at no load. Top trace, digital computer result in volts.sec. Bottom trace, test result with .25 V/div. and 5 msec./div.*

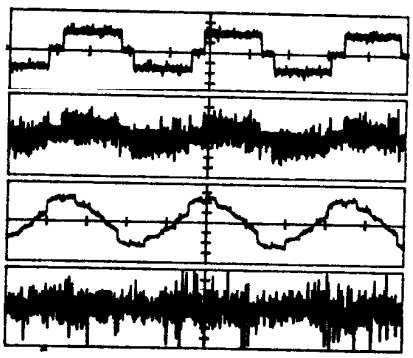

Figure 11 *Oscillogram of the five phase machine at locked rotor, rms phase current=16A, f=2.825 Hz, a) Phase current (10 A/div.), b) Line voltage (100 V/div.), c) Stator tooth flux density (.5 T/div.), d) Stator tooth search coil voltage (.2 V/div.)*

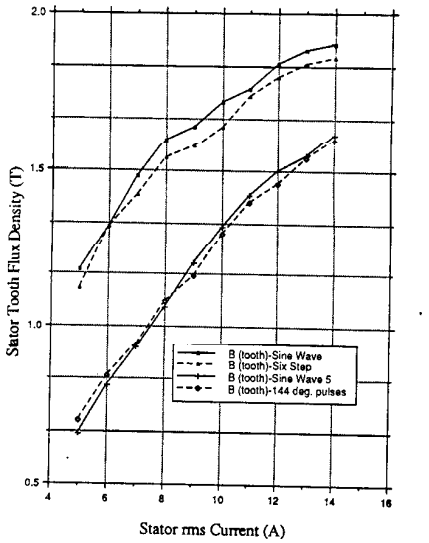

Figure 13 ***Stator tooth peak flux density variation with the total stator rms current for the three phase, four pole and five phase, eight pole induction motors with sinusoidal and quasi square waveforms supplies.***

Again to verify the validity of the simulation results presented in the previous papers [1,2], the stator phase flux linkages are calculated and compared with the experimental results. Shown in Figure 12, top trace, is the total flux linking one stator phase achieved by digital computer. The machine is under stall conditions with stator frequency of 2.825 Hz. The input current waveform is the 144 degree quasi square waveform with amplitude of about 80% of rated current. The bottom trace depicts the flux linking a pole. Notice the similarity between the measured and calculated flux waveform also, the presence of the high frequency signal due to the switching frequency in the measured oscillogram.

COMPARISON OF THE THREE AND FIVE PHASE INDUCTION MOTORS RESULTS

The result of recording the peak stator flux density at no load for three phase and five phase induction motors are illustrated in Figure 13. Shown are the plots for six step and sinusoidal waveforms for the three phase, and, 144° degree quasi square wave and sinusoidal waveforms for the five phase machines. The effect of iron saturation as stator current was increased is evidenced. It is clear that for the sinusoidal operation, the flux density is higher as it was expected. The flux density in the three phase machine is higher than the five phase due to the fact that the three phase machine has four pole and the five phase has eight pole. Therefore, the magnetizing inductance of the three phase is much larger than the magnetizing inductance of the five phase machine. The following equation presented in [4] gives the magnetizing inductance as

$$L_{ms}=\frac{N_{phase}}{4}\left[\frac{N_{turn}}{P}\right]2\ \mu_0\ \pi\ \frac{D_{is}\ l_{es}}{g'_e}\ 10^{-8}$$

where

N_{phase}	number of phases
N_{turn}	number of turns
P	number of poles
μ_0	permeability of free space
D_{is}	stator inner diameter in inch
l_{es}	stator stack effective length
g'_e	effective air-gap including the saturation

Therefore, the magnetizing inductance of the three phase, four pole induction motor is about 6.7 times, neglecting iron saturation, that of the five phase, eight pole machine. Notice that the total number of turns in both machines are the same. However, from experimental results, this ratio was determined to be about 5 due to the fact that saturation is included.

Figure 14 presents the variation of average shaft torque with the stator current variation for three phase, four pole, conventionally wound, and five phase, eight pole and four pole, concentrated winding induction motors. The five phase four pole machine is just the five phase eight pole machine which was rewound as four pole, meaning two slots per pole per phase. About 15% more torque in five phase case with respect to the three phase case for the same rms stator current is obvious. However, it is crucial to note that as it was pointed out previously the magnetizing inductance for the three phase machine is much larger than the five phase eight pole machine. Therefore for the same rms stator current, the torque producing component of the current for the three phase machine is larger than for the five phase induction motor.

CONCLUSIONS

In this paper the experimental results obtained in the lab were presented. The similarities and shortcomings between these findings and the theoretical predictions were discussed. Although two non-identical machines were examined due to the difference in the pole number in case of three phase, four pole and five phase, eight pole and slot per pole per phase number in case of five phase four pole promising results were still achieved. Also, the rather close relations between experimental results and their theoretical counter parts give us confidence in believing the simulation findings.

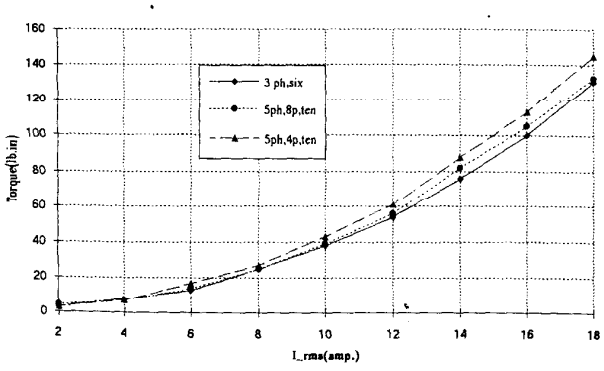

Figure 14 *Steady state shaft torque variation for three phase, four pole conventionally wound, and five phase, eight pole, concentrated winding induction motors.*

ACKNOWLEDGEMENTS

The authors wish to acknowledge the financial support provided by the Wisconsin Electric Machines and Power Electronics Consortium (WEMPEC) of the University of Wisconsin-Madison.

REFERENCES

[1] H.A. Toliyat, T.A. Lipo, and J.C. White, "Analysis of a Concentrated Winding Induction Machine for Adjustable Speed Drive Applications- part I (Motor Analysis)," IEEE Transactions on Energy Conversion, vol. 6, No. 4, pp. 679-692, Dec. 1991.

[2] H.A. Toliyat, T.A. Lipo, and J.C. White, "Analysis of a Concentrated Winding Induction Machine for Adjustable Speed Drive Applications- part II (Motor Design and Performance)," IEEE Transactions on Energy Conversion, vol. 6, No. 4, pp. 685-692, Dec. 1991.

[3] Feasibility Study of a Converter Optimized Induction Motor. Palo Alto, California; Electric Power Research Institute, January 1989, EPRI Final Report 2624-02.

[4] Analysis of Concentrated Winding Induction and Reluctance Motors for Adjustable Speed Drive Applications, Ph.D. dissertation, University of Wisconsin-Madison, Madison, Wisconsin, U.S.A.; February 1991.

[5] H.A. Toliyat, L.Y. Xue, and T.A. Lipo, "A Five Phase Reluctance Motor with High Specific Torque," IEEE Transactions on Industry Applications, vol. 28, No. 3, pp. 659-667, May/June 1992.

[6] D.M. Brod, and D.W. Novotny, "Current Control of VSI-PWM Inverters," IEEE Transactions on Industry Applications, vol. IA-21, pp. 562-570, May/June 1985.

[7] J.M.D. Murphy, and F.G. Turnbull, Power Electronic Control of AC Motors, Pergamon Press, 1988.

[8] D.W. Novotny, and T.A., Lipo, Electromechanical Systems, ECE 411, Class Notes, UW-Madison, Fall 1986.

[9] T.A. Lipo, Electromagnetic Design of AC Machines, Class Notes, University of Wisconsin-Madison.

Hamid A. Toliyat was born in Mashhad, Iran, in 1957. He received the B.S. (1982) and M.S. (1986) in electrical engineering from Sharif University of Technology, Tehran, Iran and West Virginia University, Morgantown, W.V. respectively. Between 1982 and 1984 he worked for power companies in Iran. He received his Ph.D. degree in electrical engineering from the University of Wisconsin-Madison in 1991. In 1991 he joined the faculty of Ferdowsi University-Mashhad, Mashhad, Iran, and is now an Assistant Professor of Electrical Engineering.

Dr. Toliyat is a member of the IEEE Power Engineering Society and Sigma Xi. His main research areas include converter optimized induction and synchronous reluctance machines, power electronics, power systems and control.

Thomas A. Lipo(M'64-SM'71-F'87) is a native of Milwaukee Wisconsin. He received his B.E.E. and M.S.E.E. degrees from Marquette University, Milwaukee, WI in 1962 and 1964 and the Ph.D. degree in electrical engineering from the University of Wisconsin in 1968. From 1969 to 1979 he was an Electrical Engineer in the Power Electronics Laboratory of Corporate Research and Development of the General Electric Company, Schenectady, NY.

He became Professor of Electrical Engineering at Purdue University in 1979 and in 1981 he joined the University of Wisconsin in the same capacity. Dr. Lipo has maintained a deep research interest in power electronics and ac drives for over 25 years. He has received eleven IEEE prize paper awards for his work including co-recipient of the Best Paper Award in the IEEE Industry Applications Society Transactions for the year 1984. In 1986 he received the Outstanding Achievement Award from the IEEE Industry Applications Society for his contributions to the field of ac drives and in 1990 he received the William E. Newell Award of the IEEE Power Electronics Society for his contributions to power electronics.